When interference does occur, the resulting interference area is delimited first by the guard interval duration, setting the inner limit of the interference area (the location closest to the repeater where interference impedes service) beyond which signals start falling outside the guard interval and creating interference. At this point, the interference becomes objectionable rather abruptly, as depicted in Figure 5.2.

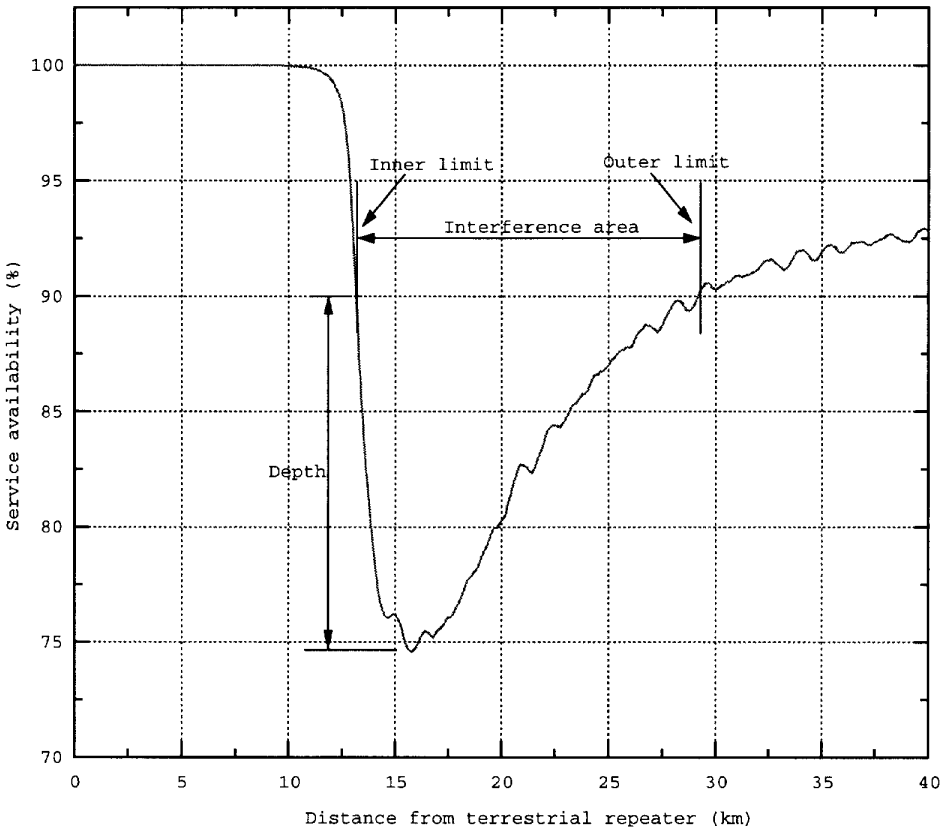

Figure 5.2: Service availability along a route from the repeater location toward the satellite.

Figure 5.2 shows a curve that corresponds to the service availability for a vehicle traveling away from the terrestrial repeater, across the interference area and eventually in the rural area served by the satellite. The service availability decreases abruptly as soon as the terrestrial signal falls outside the guard interval (i.e. at the inner limit) while near the outer limit, the service availability comes back very smoothly to the rated service objective (in this case: 90%). From this observation it can be intuitively concluded that minor changes of the repeater parameters will have an important effect on the smooth outer limit while the availability of service near the inner limit will be affected only by major changes in the broadcast system configuration (i.e., the guard interval duration). The depth of service availability in the interference area offers some interest in that it is a measure of the severity of the potential loss of service. In this case, the service availability went from 100% near the repeater down to 75%. It can also be observed that the magnitude of the interference area should be expressed not only by its surface but also by its depth.

Unlike the inner limit, the outer limit (i.e., the location furthest from the repeater where interference impedes service) does not depend on the guard interval duration, but rather on the relative repeater

signal level, such that it is still destructive with respect to the satellite signal, but sufficiently weak to meet a predetermined carrier-to-interference ratio required by the receiver. In these outer locations, the excessive radiated power from the repeater is the main cause of interference and, as seen on Figure 5.2, this interference situation improves slowly with the increase in distance from the terrestrial repeater.

In summary, the size and position of the interference area is a function of the guard interval duration and of the repeater signal energy seen by the receiver, which is, in turn, a function of the effective radiated power (ERP) and the antenna height of the terrestrial repeater. A decrease of the terrestrial repeater ERP will quickly bring in the outer limit of this interference zone whereas the inner limit will be pushed out by an increase in the guard interval duration.

The relationship between the interference area size and the ERP for various antenna heights (EHAAT: effective height above average terrain), satellite signal elevation angle and guard interval duration was investigated. Table 5.2 provides a summary identifying the conditions for which the interference area can be avoided.

EHAAT	**Mode II**		**Mode IV**	
[m]	**Elevation angle**		**Elevation angle**	
	30°	**60°**	**30°**	**60°**
25	110 W	300 W	4000 W	10000 W
50	20 W	70 W	1000 W	2300 W
100	4 W	18 W	250 W	700 W
200	< 1 W	3 W	40 W	180 W

Table 5.2: Maximum allowable effective radiated power (ERP) from the terrestrial on-channel repeater to avoid an interference area, as a function of antenna height (EHAAT), satellite signal elevation angles and guard interval duration [Mode II: 62 μs, Mode IV: 123 μs], assuming an omnidirectional re-transmit antenna.

The dominant factor is the guard interval duration. By changing from Mode II to Mode IV and thus doubling the guard interval duration (from 62 to 123 μsec), the inner limit of the interference area is pushed back further from the repeater (by a factor of 2), into an area where the potentially interfering repeater signal provides much less energy, resulting in considerably lower interference levels. It is therefore much easier to avoid the interference area with Mode IV than with Mode II.

In order of importance, the following parameters also affect the interference area: repeater antenna height (EHAAT), satellite signal elevation angle and radiated power. Of these, repeater antenna height and radiated power can be easily optimized in the design phase of the DARS network. Note the constraining limitation in ERP (4 to 18 W) for Mode II at 100 meters antenna height which would result in a very small area covered by a terrestrial repeater. In such a case, more repeaters would be needed to blanket a given area. Since the 30° elevation angle represents a worst case for CONUS coverage, the case studies reported below will concentrate on this elevation angle.

As an illustration of this approach, consider a hypothetical geostationary satellite DARS system based on the Eureka 147 modulation system operating in Mode II at L-band, with a high power omnidirectional repeater located in downtown Toronto. The ERP and EHAAT of the single repeater were adjusted to cover the metropolitan area of Toronto. This resulted in a 2000 W ERP and 200 m EHAAT. This excessive ERP, as compared to the values in Table 5.2 creates, as is to be expected, a huge interference area which has the shape of a crescent as shown in Figure 5.3 for a satellite transmission received from the South-South-West direction. In fact, Figure 5.2 could be understood as giving a profile of the interference situation for a vehicle moving from the repeater towards the direction of the satellite. By using a dozen low power omnidirectional repeaters, properly located in the city, it is possible to make the interference area disappear. This is shown in Figure 5.4, where twelve repeaters are operated at 20 W ERP and 50 m EHAAT; and the contour line indicates where the terrestrial repeaters offer coverage as opposed to the satellite. For this illustrative example, the ITU-R PN. 370 [ITU-86a] "augmented" to make it applicable to 1.5 GHz and to a 1.5 meter receiving height was used [ITU-91b].

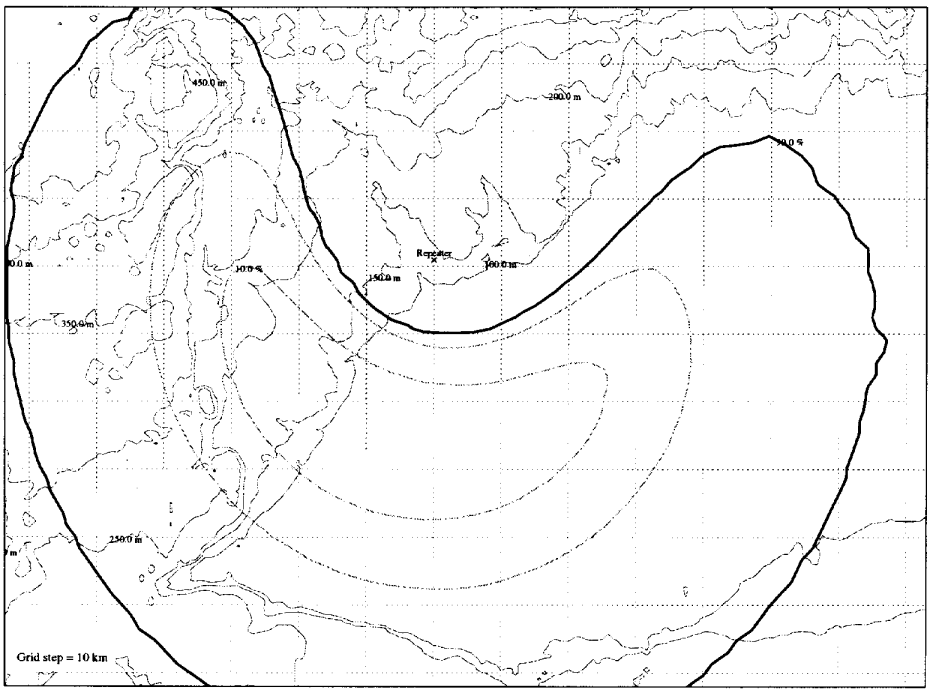

Figure 5.3: Hypothetical satellite DARS system with large interference area in the Toronto region due to excessive radiated power from the omnidirectional repeater.

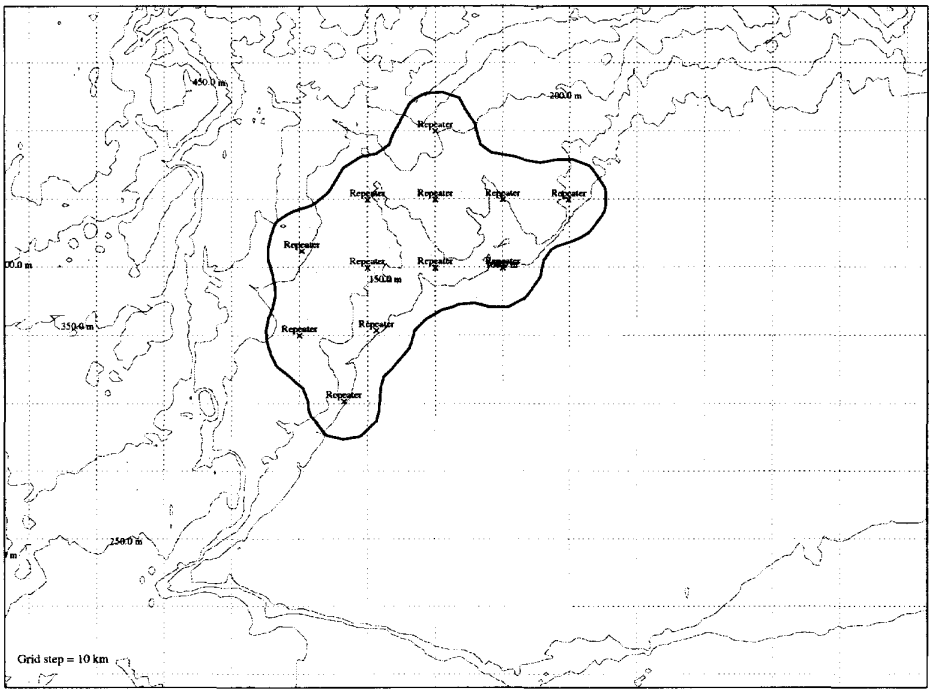

Figure 5.4: Hypothetical satellite DARS system with no interference area, using 12 well located low power omnidirectional repeaters.

Another elegant approach to avoid creating an interference area is to implement the repeaters using directional transmission antennas aimed away from the satellite and using medium power levels. This allows the use of higher power repeaters and still control the signal energy where the interference area would normally appear. Looking at the data from Table 5.2 and assuming a directional antenna with a 20 dB front-to-back ratio, the 4 W ERP limitation at 100 m EHAAT translates into 400 W ERP towards the downtown area. Although the antenna could easily provide better front-to-back ratio, this conservative value is needed in order to cover for possible back-scattering from buildings which would limit the isolation practically achievable in the field by the antenna. Such back-scattering would re-generate a local uncovered area, part of the crescent shape seen earlier in Figure 5.3, as if poorer front-to-back antenna rejection was experienced.

5.2.2 L-band and S-band coverage case study

So far, this coverage discussion was illustrative in order to explain the satellite/terrestrial interference phenomenon. A second example is now considered, this time based on a generic scenario to develop a comparison between what can be achieved at L-band and S-band. The target coverage area is a polygon of approximately 30 km by 50 km (i.e. representative of a coverage areas similar to metropolitan Toronto shown in Figure 5.2 and 5.3) and consisting of dense urban, urban, suburban, industrial and other types of areas.

Based on information provided in Section 3 of this report, it seems safe to assume that by using S-band frequencies instead of L-band frequencies, a penalty of typically 6 dB in satellite transmission power can be expected due to purely propagation and receiving antenna aperture considerations. Similarly, a 10 dB penalty is expected in the case of the terrestrial transmission for a 95% service availability.

Another important factor is the Doppler spreading of the signals due to vehicle displacement. Figure 5.5 presents computer simulation results showing the impact of Doppler spread in the worst case condition of a typical urban channel as defined in the COST 207 model [COS-89], seen as a degradation of system performance in E_b/N_o as a function of vehicle speed for Modes II and IV for a BER of 10^{-4}. The abscissa provides two different scales, one for L-band and one for S-band. This is based on the fact that Doppler spread is a linear function of both carrier frequency and vehicle speed. A multiplication factor of 0.63 (i.e. 1.472 GHz/2.335 GHz = 0.63) is used to scale the vehicle speed from L- to S-band. Environment types other than urban are not presented here because the urban environment will be the most critical as far as satellite signal outage, which is the reason why terrestrial on-channel repeaters are considered at all.

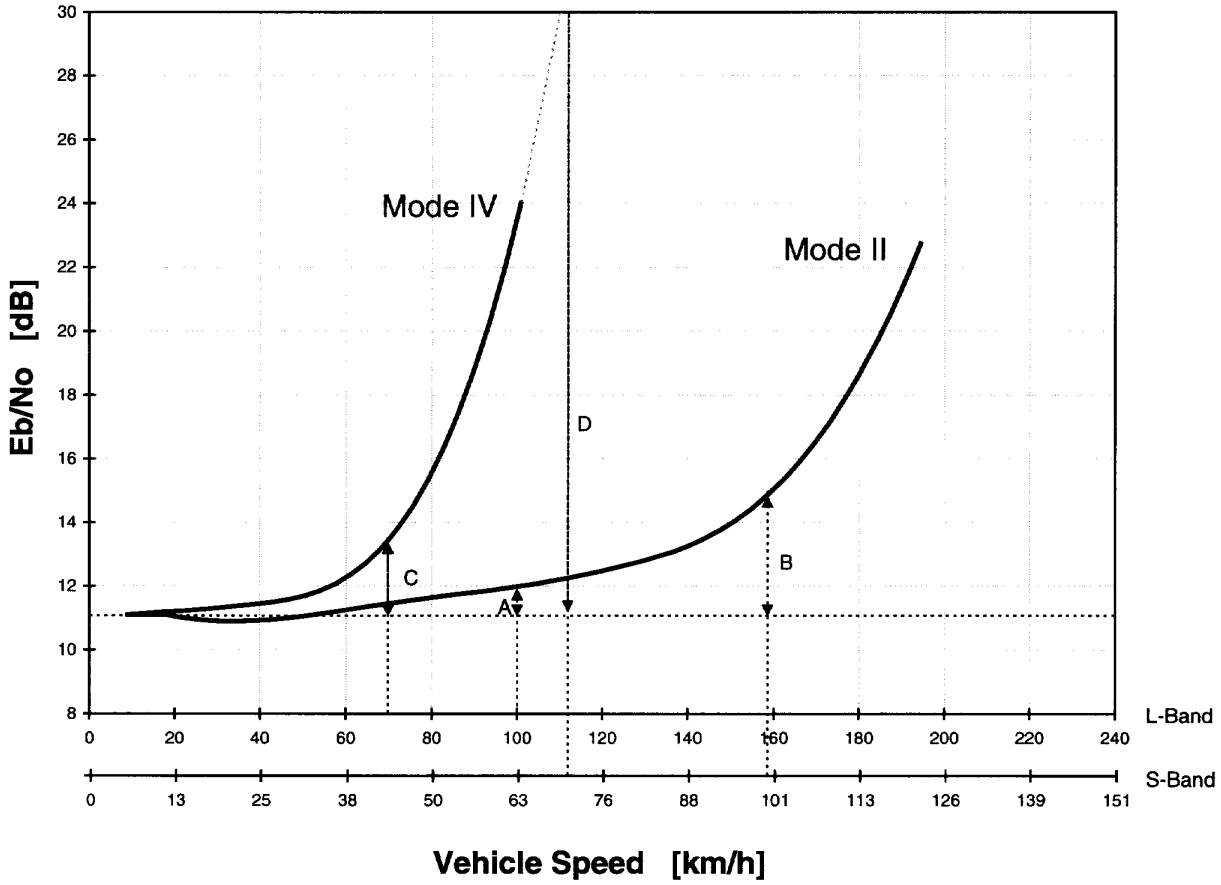

Figure 5.5: Impact of Doppler spread on Eureka 147 DAB system performance at a BER of 10^{-4} in Modes II and IV for the typical urban channel defined in COST 207, as a function of vehicle speed scaled for L- and S-bands.

Two scenarios will be developed here assuming a reference maximum vehicle speed of 70 km/h, in an urban environment, used for the purpose of comparison between L-band and S-band. This speed is used as a reference point for comparison purposes. As can be seen from Figure 5.5, 80 km/h is still comfortable as a maximum vehicle speed in Mode IV at 1.5 GHz for such an urban environment

It should be noted that for these two case studies, it was found more appropriate and accurate to use the Okumura-Hata urban propagation model which is based on extensive empirical data from measurements in urban environments, unlike in the illustrative case where the ITU-R PN. 370 propagation curves were used to model the suburban and rural propagation in the South-West area of

Toronto. This more realistic model has the merit of being based on measurements made in typical vehicular reception conditions and also being scaleable in frequency at L-band and S-band.

The first case study is an example of a L-band system using Mode IV with an impact of 2 dB on the terrestrial link budget due to spectrum spreading at a BER of 10^{-4}. The coverage of the hypothetical area of 30 km by 50 km for this system example is given in Figure 5.6 where, as can be found in Table 5.2, 250 W omnidirectional repeaters can be used for a EHAAT of 100m.

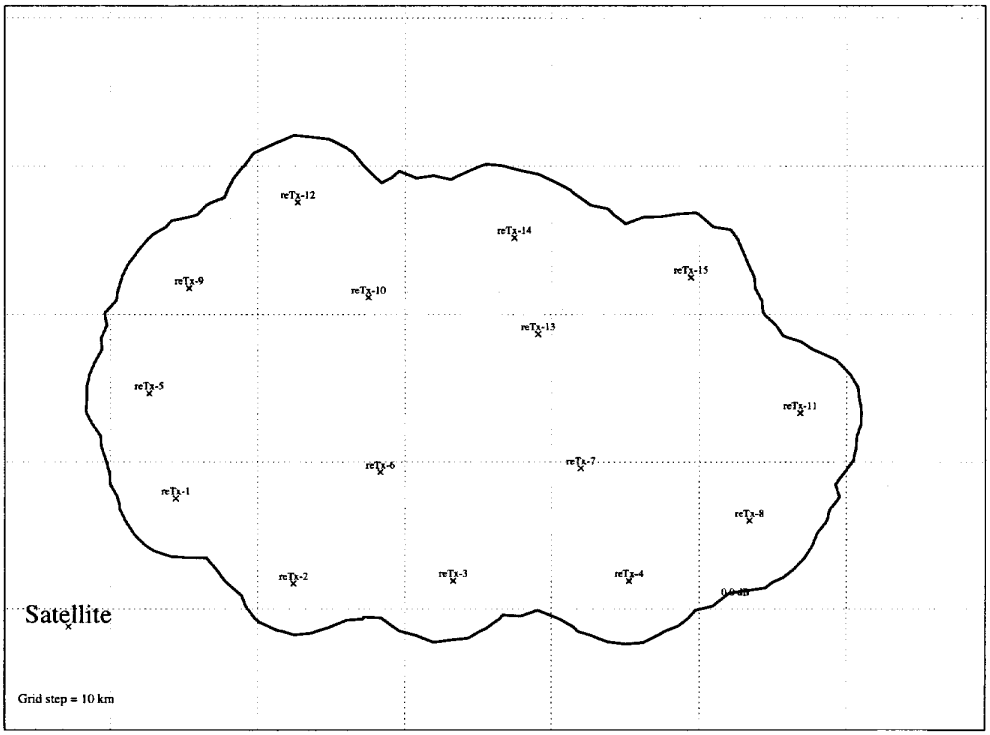

Figure 5.6: Service coverage of a predetermined area for L-band (Eureka 147 system in Mode IV) requiring 15 omnidirectional repeaters of 250 W ERP each at 100 m EHAAT.

These results are similar to those obtained in the Toronto case where 12 repeaters were required, using a different set of assumptions (Mode II, ITU-R PN. 370 model, 50 m EHAAT, etc.). Now, by applying a more refined system design approach, it is possible to substantially decrease the number of repeaters. Figure 5.7 shows the same situation but this time directional antennas are used yielding an equivalent coverage with only four (4) repeaters. This is explained by the fact that directional antennas with 20 dB front-to-back ratio potentially allow an increase of the ERP from the value indicated in Table 5.2 up to a value of 20 dB higher. In this case, the EHAAT was maintained at 100m but the ERP was increased to 12 kW which is 3 dB less than the maximum allowable ERP of 25 kW.

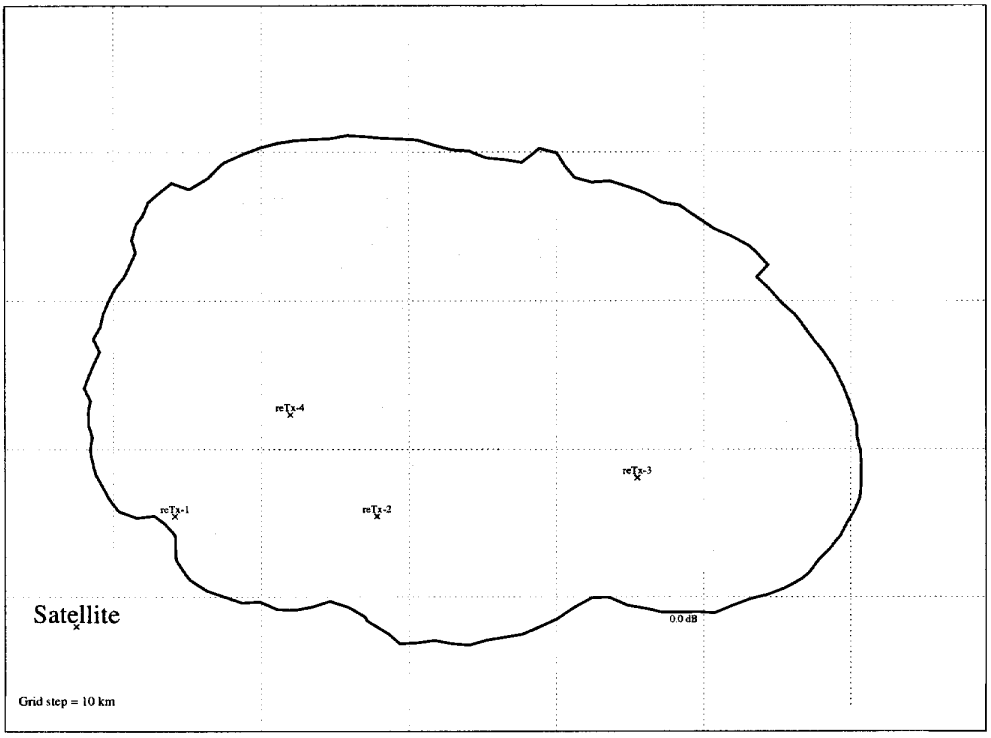

Figure 5.7: Service coverage of a predetermined area for L-band (Eureka 147 system in Mode IV) requiring 4 directional repeaters of 12 kW ERP each at 100 m EHAAT.

The second case study is at S-band. To be able to keep the same vehicle speed of 70 km/h, the symbol period and the guard interval (GI) duration need to be scaled down by a factor of 0.63 (relative to L-band in Mode IV) therefore reducing the guard interval from 123 μsec to 77.5 μsec. Mode IV could not be used in this case because the impact of Doppler spread on the terrestrial link budget would be too important: the vehicle speed would have to be limited to about 50 km/h to limit the impact on the required Eb/No to 4.5 dB as seen in Figure 5.5. At higher vehicle speeds, this impact would increase exponentially. Mode II could be used at S-band but, in order to be able to make a strict comparison between the two frequency bands, the proportional scaling of the guard interval was retained.

The maximum allowable ERP for 100 m EHAAT, at S-band, had to be interpolated from values in Table 5.2 between 4 W (GI = 62.5 μsec) and 250 W (GI = 123 μsec) for the scaled guard interval of 77.5 μsec needed at 2.3 GHz. This was done by first estimating the field strength at which the interference problem starts occurring for Mode II and Mode IV, at L-band. Figure 5.8 shows the field strength as a function of distance for three transmitters; two are at L-band and one is at S-band. The propagation model used here is the same as the one used to create Table 5.2 for 95% coverage availability. In Mode II, the interference zone starts at around twelve kilometers from the repeater, for a 30 degree elevation angle. Looking at the 4 W ERP curve on Figure 5.8, the corresponding field strength is 35 dBμV/m. In Mode IV, the interference zone starts at around 24 km. The 250 W ERP curve shows that for a level of 35 dBμV/m, the distance is indeed 24 km. The third curve was found using the same propagation model but scaled for a 2.3 GHz operation in a rural environment and the point of interest is the intersection of the 35 dBμV/m field strength with the distance of 15.2

km (i.e., 0.63 x 24 km = 15.2 km). The corresponding ERP value is what is considered to be the maximum allowable ERP for an omnidirectional repeater at S-band to avoid satellite/terrestrial interference problem. This value is in the order of 20 W. Furthermore, the field strength at which the interference zone would start to appear would be 6 dB higher than in the 1.5 GHz case since the satellite transmission power has to be increased to compensate for the smaller receive antenna aperture and increased propagation losses as indicated in section 4.3.7. This being known, the simulations can then be performed using either 80 W omnidirectional repeaters or directional repeaters with an ERP of up to 8 kW.

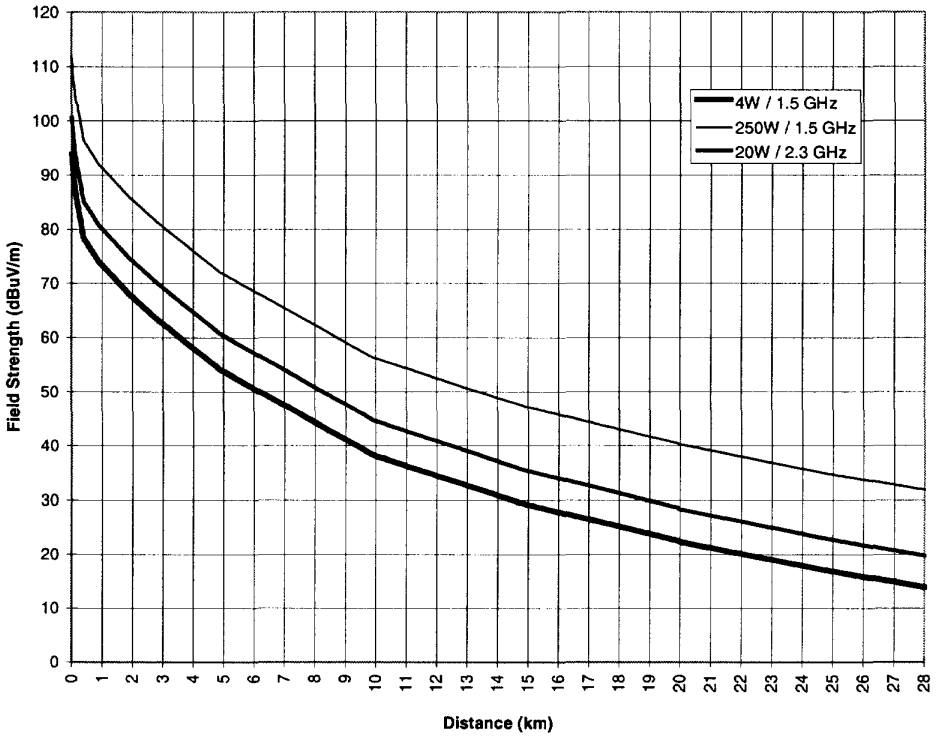

Figure 5.8: Field strength as a function of the distance from the repeater. Three ERP values are shown, 250 W and 4 W at L-band and 20 W at S-band.

At S-band, a penalty of 10 dB due to propagation effects for terrestrial transmission in urban environment, as explained in section 4.3.7, was taken into account in generating the coverage depicted in Figure 5.9. Eighty-five (85) repeaters are now necessary. The high density is mostly due to the propagation losses but another important limiting factor is the interference that the second and third row of transmitters causes to the first row, and so forth. This represents a considerable increase (by a factor of 5.7) in the complexity of the infrastructure, as well as the operations and maintenance costs, when compared to L-band.

Since the previous coverage exercise at L-band demonstrated the benefits of using directional antennas, a coverage exercise was repeated at S-band with repeaters equipped with directional antennas with 20 dB front-to-back ratio. This created a network of 9 directional repeaters operating at ERP of 8 kW, as shown in Figure 5.10.

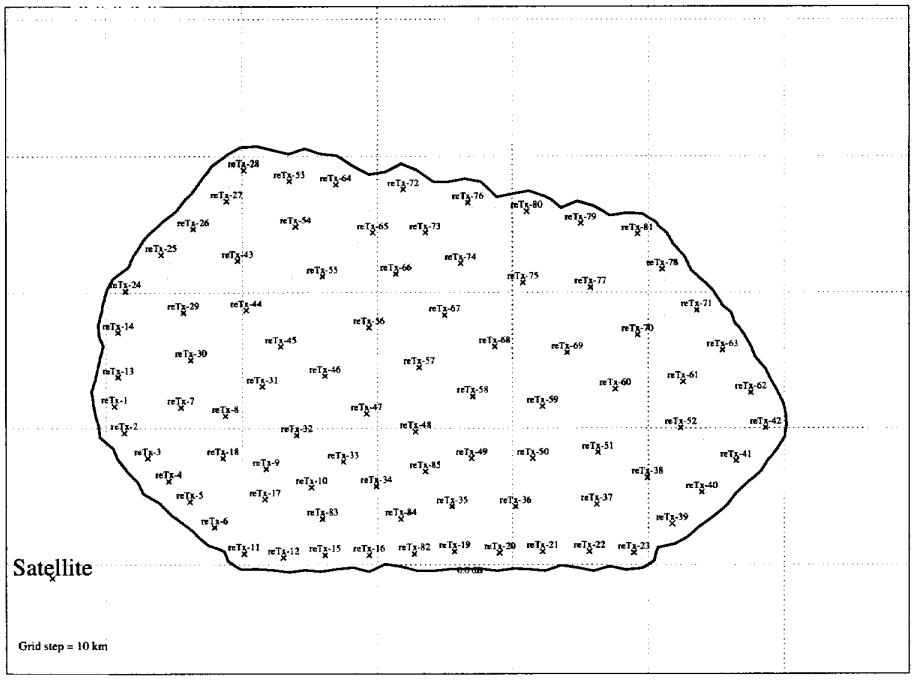

Figure 5.9: Service coverage of a predetermined area for S-band (Eureka 147 system) requiring 85 omnidirectional repeaters of 80 W ERP each at 100 m EHAAT.

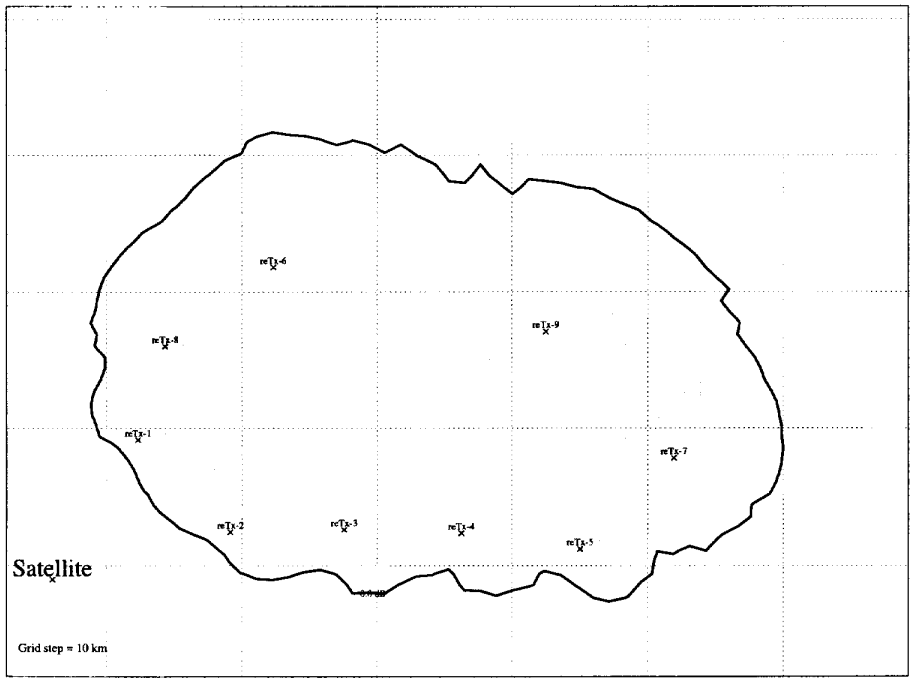

Fig. 5.10: Service coverage of a predetermined area for S-band Eureka-147 requiring 9 directional repeaters of 8 kW ERP each at 100 metres EHAAT.

These coverage simulations have illustrated the various extent of difficulty in implementing hybrid repeaters, whether in L-band or S-band. It appears clear that the S-band implementation is more difficult due to its large complexity shown by the number of repeaters required but, less evidently, by the difficulty in achieving proper coverage while controlling the effect of the multitude of destructive active echoes generated by this large number of repeaters

This comparison has been useful in determining a relative increase in the system complexity when using two different frequency bands. This was done by establishing a reference set of parameters which were scaled from L-band to S-band to minimize the number of variables that would affect the comparison. This should not be seen as an absolute answer to the presented theoretical coverage area (flat terrain with no blockage but still assuming the Okumura-Hata urban fading model). In an actual system implementation, the designers should be able to take advantage of the local terrain features and buildings to minimize the interference between repeaters and possibly reduce somewhat their required number. Never-the-less, the ratio in complexity between the two bands is likely to stay close to constant.

6. Single carrier modulation

Single carrier modulation is the other main candidate modulation for DAR systems required to operate in a hybrid satellite/terrestrial environment.

6.1 Proposed single carrier DARS systems

Of the four systems that have been proposed to the FCC to provide domestic DARS services via satellites in the US, three use a single carrier QPSK modulation. Those are the AMRC [AMR-92], Primosphere [PRI-92] and the CD Radio [CDR-92] systems. The fourth DARS system (DSBC) submitted to the FCC will not be considered here since it uses a transmission scheme based on spread spectrum techniques. The characteristics of the channel coding and modulation of these three systems are summarized in Table 6.1. Also shown in this table are the characteristics of the transmission schemes of two other systems that have been developed and proposed for DARS. The first one is the VOA/JPL system [ITU-95b] which has been submitted to and tested by the EIA/CEMA DAR Subcommittee [EIA-95] at 2 GHz. The second one is the WorldSpace system [SAC-97] which is to provide, at L-band (1452-1492 MHz), a satellite digital audio broadcast service to major parts of the world (Africa, the Middle East, Asia Pacific, Latin America and the Caribbean) by the next millennium.

Listed in Table 6.1 are the key parameters that affect the spectral and the power efficiency of the transmission. The information contained in this table is based on open sources and conversations with the proponents and reflects the best available information at this time. It should be emphasized that some of the parameters of this table are likely to change once the rules governing satellite DARS have been established and laboratory and/or field tests have been conducted. This is especially true for the two DARS systems to which spectrum has been auctioned by the FCC (AMRC and CD Radio). The VOA/JPL and WorldSpace are in an advanced state of development and have even been tested in hardware [EIA-95, SAC-97].

All of the systems listed in Table 6.1 proposed using QPSK (Quadrature Phase Shift Keying) modulation or its variant OQPSK (Offset QPSK). This choice is motivated by the fact that QPSK is

a good compromise between spectral and power efficiency, the latter being a prime factor for satellite transmission. The other important consideration for QPSK is that this modulation provides negligible fluctuations in the signal envelope which allows for the satellite power amplifiers to be operated near saturation.

The VOA/JPL and the WorldSpace systems rely on coherent demodulation to optimize power efficiency. Although details on the type of demodulation of the other three systems were not available, coherent demodulation will also likely be used to reduce the power requirements to its minimum (3 dB advantage in satellite power). When the mobile receiver is in line-of-sight with the satellite, the resulting Rician channel provides a stable direct signal and carrier phase estimation and tracking can be performed efficiently with phase-locked loop based techniques [PRO-89]. However, when the mobile receiver is in shadowed areas, a situation which would occur frequently in urban areas, no direct signal is available and the received signal consists of multipath components which can be strongly faded. In such Rayleigh faded channels, coherent demodulation requires the periodic transmission of pilot tones or pilot symbols along with the data symbols [DAN-94, CAV-92, MOH-89]. This extra information reduces the spectral efficiency of the transmission.

Parameter	AMRC	Primosphere	CD Radio	VOA/JPL	WorldSpace
Modulation	QPSK	OQPSK	OQPSK	QPSK	QPSK
Demodulation	NS	NS	NS	Coherent	Coherent
FEC type	Convolutional	Convolutional	Convolutional	Concatenated Convolutional + Reed-Solomon	Concatenated Convolutional + Reed-Solomon
FEC code rate	1/2	1/4	1/4	Convolutional: ½ Reed-Solomon: 140/160	Convolutional: ½ Reed-Solomon: 223/255
FEC decoding	NS	Viterbi	Viterbi	Viterbi	Viterbi
Useful bit rate	220 kbit/s[1]	1.536 Mbit/s	3.97 Mbit/s	190 kbit/s[2]	1.541 Mbit/s
Raw bit rate	440 kbit/s	6.144 Mbit/s	15.88 Mbit/s	440 kbit/s	3.535 Mbit/s
Signal bandwidth	220 kHz	3.072 MHz	8 MHz	220 kHz	1.767 MHz
Equalization	NS	NS	NS	yes	no
Diversity	NS	NS	Transmission	Transmission Reception	no

NS = Not Specified in sources available

Note 1: Little information on the transmission scheme of the AMRC system is available. Four channel types are defined in [AMR-92] which have bit rates ranging from 9.6 to 220 kbit/s. No mention is made of any multiplexing of these channels into a composite data stream. A single 220 kbit/s channel is assumed in this table.

Note 2: The VOA/JPL system description in [ITU-95] specifies that various audio and ancillary data sources can be multiplexed into a composite serial data stream with a bit rate ranging from a minimum of 32 kbit/s to a maximum of 1 to 10 Mbit/s. The parameter values shown in Table 1 correspond to a system configuration similar to the one tested in the EIA-CEMA/NRSC DAR Subcommittee tests [EIA-95].

Table 6.1: Proposed single carrier satellite DARS systems

Three systems use a convolutional code alone and two use a concatenated convolutional/Reed-Solomon code which usually yields a more powerful code. The optimal Viterbi algorithm is used by most systems to decode the convolutional code.

With respect to data throughput and signal bandwidth, the systems can be classified as narrowband (signal bandwidth around 200 kHz) or wideband (signal bandwidth greater than 1.5 MHz).

One DAR satellite system (VOA/JPL) is claimed to have been designed to allow the optional use of equalization if gap-fillers are operated to support and complement satellite delivery. Two systems (VOA/JPL and CD Radio) have provision to use two widely spaced satellites to provide transmit

diversity. The VOA/JPL system has also provision for the use of two receive antennas to provide space diversity at the receive end.

6.2 Adaptive equalisation techniques

Multipath introduces interference between adjacent symbols which is known as ISI (intersymbol interference). In open and rural areas, where the received direct (line-of-sight) satellite signal dominates the weaker multipath signals, ISI is minimal and satisfactory performance can be obtained with a good error correction code coupled with time interleaving. This is especially true for satellites at relatively high elevation angles. In dense urban areas however, shadowing by buildings will block the satellite signal and the only way to deliver a sufficiently strong signal to the receiver in this environment is through the use of terrestrial gap-fillers (see Section 4.4.3). In these conditions, a direct signal is rarely available and the received signal is composed primarily of multipath components which can cause severe ISI . An error correction code alone will be insufficient for single carrier systems to cope with this strong ISI. Additional multipath mitigation techniques, such as equalization, are thus required.

6.2.1 Types of equalization techniques

Equalization techniques for combating ISI on band limited time dispersive channels may be divided into two general types - linear and nonlinear equalization. Associated with each type of equalizer are one or more implementation structures. Furthermore, for each structure there is a class of algorithms that may be employed to adaptively adjust the equalizer parameters according to some specified performance criterion. Figure 6.1 (after Proakis [PRO-91]) provides an overall categorization of adaptive equalization techniques into types, structures and algorithms to adaptively adjust the equalizer parameters according to some performance criterion.

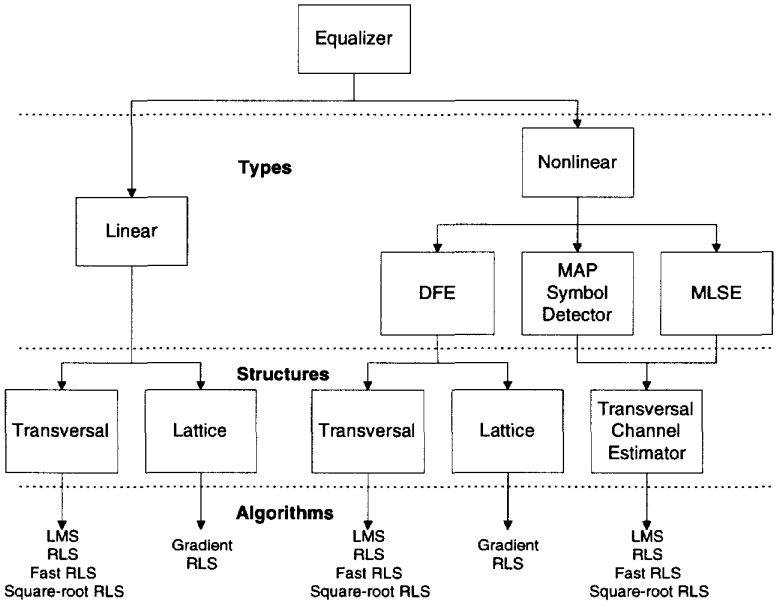

Figure 6.1: Equalizer types, structures and convergence algorithms [PRO-91]

The linear equalizer has been widely used for equalization of telephone channels. Usually, a transversal (tapped-delay-line) filter structure is employed, with tap weight coefficients that are adjusted adaptively using the gradient type LMS (least mean square) algorithm due to Widrow and

Hoff [WID-60]. The taps are spaced at the data symbol duration T, or some fraction of it. Viewing the transmission channel as a filter, the linear equalizer attempts to synthesize an inverse filter which compensates for the distortion introduced by the channel. This works well for some types of distortion, but on channels which have spectral nulls in their frequency response, the linear equalizer yields very poor error rate performance. The reason for this is that the linear equalizer attempts to compensate for the null by introducing a high gain at that frequency. This compensates for the channel distortion at the expense of enhancing the additive noise. Since this kind of channel characteristic is often encountered on mobile (time-varying) multipath channels, the linear equalizer is unsuitable for equalization of such channels [PRO-89].

Nonlinear equalizers find use in applications where the channel distortion is too severe for a linear equalizer to handle. Three nonlinear equalization methods have been developed. One is the decision feedback equalization (DFE). The second is the symbol-by-symbol detection algorithm based on the maximum *a posteriori* probability (MAP) criterion proposed by Abend and Fritchman [ABE-70]. The third is the maximum-likelihood sequence estimation (MLSE), which is usually implemented by means of the Viterbi algorithm [FOR-72]. The MLSE is the most effective demodulation (or detection) technique (optimum in the sense of minimizing the probability of a sequence error) for digital signals corrupted with ISI and noise [FOR-72, UNG-74]. Despite its effectiveness, the high computational complexity of the MLSE technique limits its application. The MLSE also has problems tracking rapidly varying channels, due to the delay inherent in the Viterbi algorithm data detection process. In practice, the MLSE technique is used only when the ISI extends over only a few symbol intervals, since its computational and storage requirements increase exponentially with multipath spread. (Complexity of MLSE is proportional to M^L, where M is the size of the data symbol alphabet and L is the number of symbols spanned by the ISI.) The MAP equalizer has similar complexity to the MLSE. Consequently, linear equalizers and decision-feedback equalizers (DFE) are most common [PRO-89, PRO-79, AUS-67]. When the channel introduces deep spectral notches and ISI is spanning many symbols, the DFE is essentially the only feasible choice.

6.2.2 Decision-feedback equalizers

A key issue with any equalizer is the algorithm used to set its coefficients, and in the case of time-varying channels, the coefficients must be updated quickly enough to track the changes in the channel characteristics. The most common algorithms which have been applied to DFE designs are outlined below.

6.2.2.1 DFE structures

As shown in Figure 6.1, within the class of decision feedback equalizers, there are two basic structures and several algorithms used for convergence and tracking. The classic DFE structure includes two finite impulse response (FIR) transversal filters, distinguished as the feedforward filter (FFF) and the feedback filter (FBF), combined with a symbol detector (usually a threshold device). The taps of the FBF are typically spaced at the symbol duration T. The tap spacing of the FFF may be T but it is usually decreased to T/2, which markedly reduces the sensitivity of the DFE to timing errors. Generally, the FFF reduces the ISI at the sampling instant caused by the "future" symbols, i.e., those which follow the present symbol, while the feedback filter suppresses the ISI components induced by the "past" symbols, i.e., those already detected before the current symbol

As shown in Figure 6.1, there is a also a lattice structure for the DFE, and a corresponding family of algorithms developed for use with this structure. The lattice forms have been shown to have some performance advantages over the conventional RLS DFE, at the cost of greater complexity; one in particular, the lattice predictive DFE [LIN-86], has the interesting property that the length of its

feedback section can be changed in real time without affecting normal operation. This could be advantageous in mobile channels where the multipath delay spread is subject to large changes such as in the case of an hybrid satellite/terrestrial operation, since the performance of the DFE degrades if the length of the FBF is not matched closely to the impulse response of the channel.

6.2.2.2 DFE algorithms

The algorithms used to adjust the DFE coefficients can roughly be classified into two categories: the simple but slow and the fast but complex methods. Early designs used the LMS algorithm, mentioned above in connection with linear equalizers. However, the LMS algorithm is unsuitable for tracking channels with rapid fading, since its convergence rate is relatively slow, and it becomes even slower when the channel has spectral nulls or near nulls. The RLS (recursive least squares) family of algorithms has much better convergence rates (often by an order of magnitude or more) than the LMS. The various RLS algorithms differ considerably in complexity and performance, with the fast RLS (Kalman) algorithm being perhaps the most popular due to its relative simplicity.

An important component of most DFE designs is the provision for periodic insertion of a known sequence of symbols in the transmitted signal in order to train the equalizer. Although much research has been done on "blind" equalization in which no knowledge of the transmitted signal content is assumed, the most successful DFE implementations to date all seem to make use of training sequences. This of course represents overhead which reduces the maximum useful data rate, but as is the case with the guard interval in COFDM, this overhead is necessary if useful BERs are to be achieved. The length of the training sequence is dictated by the length of the channel impulse response (CIR) and the speed of convergence of the DFE adaptation algorithm. A slower algorithm will require more training overhead; moreover, in a rapidly time-varying channel, the CIR could change significantly during the training sequence. In this case, the algorithm will never converge, and the DFE will fail.

In the classic DFE, the equalizer coefficients are adjusted sequentially, symbol by symbol, during the tracking phase between training sequences. Recent attention has focused on a new class of DFE algorithms in which equalization is applied to blocks of received data (block DFE, or BDFE) [HSU-85, CRO-89]. In the BDFE, a block of data symbols is surrounded by blocks of known training symbols. A recursive data detection technique to decode the data symbols in pairs, starting with the first and last symbols in the data block, is commonly used. Once these decisions are made, these are then treated as known data and the data detection process is iterated to make decisions on the subsequent edge symbols until the entire block of data has been processed. The computational complexity of BDFE is significantly less than the RLS DFE for equalizer lengths of 10 or more taps [DAV-88]. BDFE's are consequently particularly well-suited to fast-fading channels; on HF channels, they have been shown to deliver useful BER performance at fading rates well beyond the point at which the conventional RLS DFE collapses.

6.2.2.3 DFE Implementation issues

The complexity of a DFE implementation is usually specified in terms of the number of complex multiplications which must be performed for each received symbol. For a given symbol rate, this gives a good indication of the computing horsepower required for that implementation. The main determinants of complexity are the particular algorithm used, and the number of taps in the DFE. The latter quantity is directly related to the multipath delay spread of the channel (i.e., the number of symbol periods spanned by the CIR). The complexity of the algorithms for adaptation of the DFE varies greatly, but as mentioned above, the less complex algorithms tend to converge too slowly to be useful in rapidly varying channels. Of those which do converge more quickly, many have stability

problems. Rather than attempting to compare all of the possibilities, we focus here on one of the most promising candidates, the BDFE. In particular, we considered a BDFE design developed at CRC for HF applications, which has been shown to outperform more traditional DFE implementations in fast fading situations, yet is less complex than some of the earlier sequential designs.

The signaling format of the BDFE is shown in Figure 6.2. The complexity of the BDFE is a function of two parameters: N_{ct}, the span of the *channel tracker* in symbol periods, and D, the number of symbols in the data block. N_{ct} must be long enough to span the CIR and D is dictated by the maximum fading rate of the channel. The length N_t (in multiples of the symbol period T_s) of the training block or *channel probe* sequence also depends on N_{ct}:

$$N_t \geq 2N_{ct} - 1$$

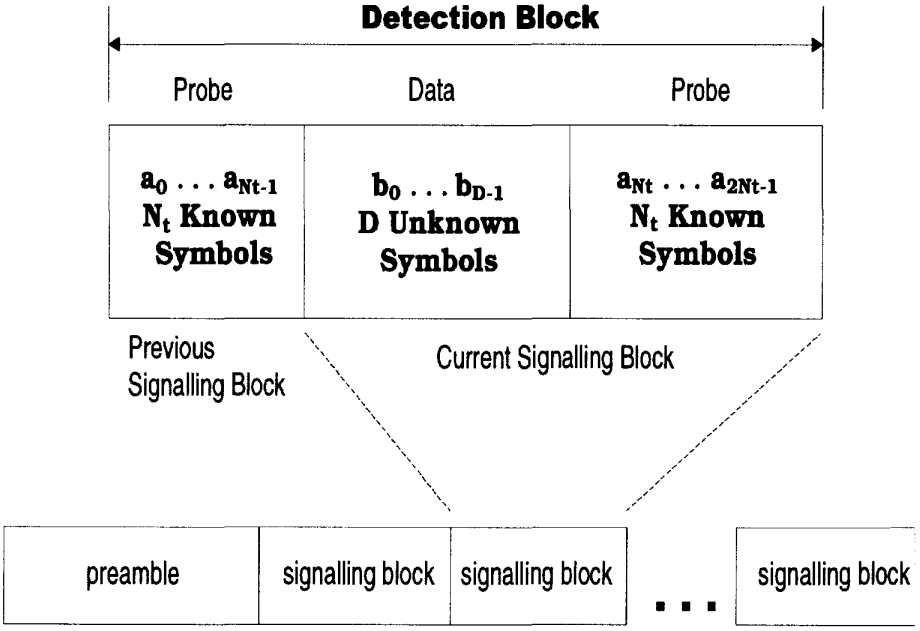

Figure 6.2: BDFE Signaling Format

The *correlation time* (also known as *coherence time*) of the channel is equal to the reciprocal of the Doppler spread, and the interval between training blocks, set by D, should be considerably less than this for best results from the BDFE. This creates a fundamental limitation: as the Doppler spread increases, more and more of the signal waveform must be dedicated to CIR estimation, until the point at which no useful throughput remains. Again, this is analogous to the situation in COFDM where Doppler spread becomes the limiting factor in performance at some point. For this BDFE implementation, there is a simple relationship between the probability of bit error P_b, the time between channel probes T_t (i.e., N_t + D symbol periods), and the channel correlation time T_c (only valid when the SNR is high):

$$P_b = k(T_t / T_c)^4 = k[(N_t + D)T_s / T_c]^4$$

where k is a constant of proportionality which depends on the type of modulation used. The factor k is approximately 0.6 for QPSK, 3 for 8PSK, and 10 for 16QAM. It can be seen that for a BER of the order of 10^{-4}, the interval between channel probes should be no more than about 10% of the correlation time.

The complexity of the BDFE as a function of N_{ct} for four values of D is shown in Figure 6.3.

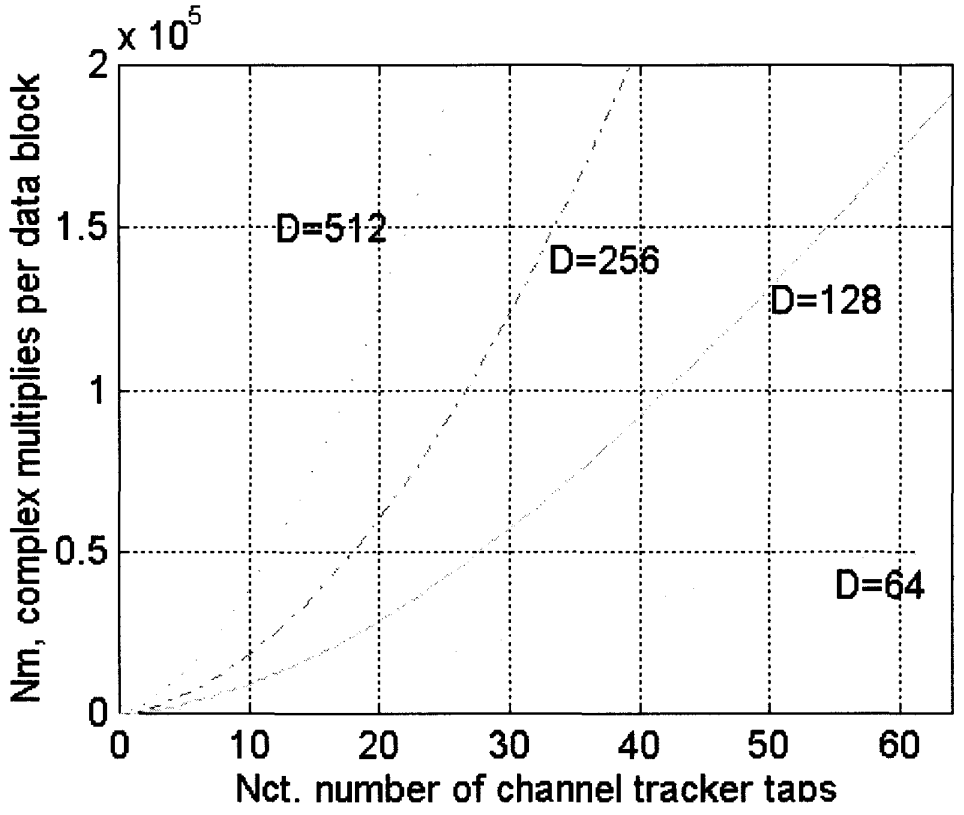

Figure 6.3: Complexity of BDFE Implementation

6.3 Case study for single carrier modulation

6.3.1 Channel characteristics

One important consideration when using channel equalization is that this feature is beneficial only if the received signal is selectively faded in frequency, which implies that only part of the received signal spectrum is faded. If the received signal is flat faded, then equalization provides no benefit. Before considering the use of equalization, it is therefore relevant to examine the coherence bandwidth of the radio channels in which transmission will take place or, equivalently, the multipath delay spread, since the two parameters are inversely proportional (see Section 4.5.2).

The environment created by satellite transmission complemented with on-channel repeaters is quite unique with respect to multipath. The presence of "active" echoes generated by the repeaters results in a wide range of multipath delay spreads. In Section 4.4.4, it was shown that, depending on receiver position relative to the repeaters, multipath delay spread can range from small values (less than 1 μsec), in open rural areas remotely located from repeaters, to several tens of microseconds when the receiver is within range of multiple transmitters. The measured delay spread values

reported in Section 4.5.2 for a single terrestrial transmitter would also be expected to occur in areas close to a repeater. To the authors' knowledge, no statistics derived from measured data exist, to characterize the multipath delay spread in a satellite/repeater or a multiple transmitter environment.

This wide range of delay spreads represents a challenging situation for an equalizer which would require, in some cases, a large number of taps. Moreover, the equalizer would be required to constantly adapt not only its **coefficient values** to track the time variations of the channel, but also the **number of coefficients** to track the multipath delay spread changes of the channel. For optimal performance, the time span of an equalizer should match the impulse response duration of the channel.

6.3.2 Case study guidelines

Based on the characteristics of proposed satellite DARS systems (Table 6.1), two classes of single carrier systems can be defined. These are the **single service systems**, which would provide a single CD quality audio service possibly combined with some ancillary data, and the **multi-service systems**, which would provide several audio services again possibly combined with ancillary data. The single service systems would typically require a signal bandwidth in the neighborhood of 200 kHz while the bandwidth of multi-service systems could range from 1.8 to 8 MHz.

In the case studies below, the single and multi-service DARS systems are referred to as *narrowband* and *wideband* single carrier systems respectively. The feasibility of using equalization with both narrowband and wideband single carrier modulation is assessed in terms of useful data throughput and equalizer implementation complexity. The analysis is done both at L-band and at S-band. A signal bandwidth of 220 kHz (equivalent to that of the VOA/JPL system) and 1.767 MHz (equivalent to that of the WorldSpace system) is assumed for the narrowband and the wideband systems respectively. The maximum multipath delay spreads that the equalizer is expected to handle are similar to those values used in the multi-carrier modulation case study (Section 5.2). For convenience, we used 64 and 128 μsec here, which differs only slightly from the multi-carrier case. The BDFE structure described in Section 6.2.1 will be used, since it represents the state of the art in equalization and is a technique well-suited to fast fading channels. A reference vehicle speed of 100 km/h is assumed. Complexity of the BDFE is assessed in terms of the number of complex multiplies per second which must be performed. The estimated DSP capacity needed to implement the equalizer is based on performing these operations, plus additional overhead to cover BDFE setup and calculation of the CIR estimates. The overhead is in the 25% to 50% range for the cases shown in the following two sections.

6.3.3 Case study: narrowband single carrier system

For this case, we consider a system which carries a single stereo service, plus some capacity for ancillary data. The basic system characteristics are modeled on the VOA/JPL system, as summarized in Table 6.1. For the four different combinations of frequency and maximum delay spread under consideration, Table 6.2 shows the various parameters which lead to an estimate of the complexity of a BDFE implementation for each case. A channel BER of 10^{-2} is assumed to be required at the output of the equalizer. Also shown is the efficiency, which is the percentage of transmitted symbols carrying useful data, and the data throughput after the overhead for both CIR estimation and error correction coding are taken into account.

It is perhaps slightly surprising that the S-band realization of the equalizer would require approximately the same computing power as the L-band case. The dominant factor in determining equalizer complexity is the number of taps, which is a function of the symbol length and the

maximum delay spread, both of which are assumed to be the same for the two bands. The higher maximum Doppler shift in the S-band case manifests itself in the need for more frequent sampling of the CIR; this results in reduced efficiency and reduced overall throughput, but it also reduces by a small amount the number of calculations needed per unit time. Note that the throughput is on the low side for carrying both CD quality stereo audio and data services, especially in the S-band case with longer delay spread. This could be addressed by increasing the symbol rate, but at the cost of further complicating the equalizer implementation. Another option would be to go to 8PSK modulation, but the SNR penalty in doing so might be unacceptable in terms of the satellite link budget. Note also that if the target BER was required to be lower than 10^{-2}, the efficiency and throughput would drop accordingly (however, with the powerful coding assumed in this case study, 10^{-2} BER is ample).

	L-Band		S-Band	
Max delay spread, μs	64	128	64	128
No. of equalizer taps (N_{ct})	15	29	15	29
Symbols/channel probe block (N_t)	29	57	29	57
Max. Doppler shift, Hz (@ 100 km/h)	134		213	
Correlation time, ms (T_c)	7.45		4.54	
Correlation time / symbol time (T_c / T_s)	1641		1035	
Channel sampling interval, symbols(N_t+D)	492		310	
Data block size, symbols (D)	463	435	281	253
Efficiency, % [Note 1]	**94.1**	**88.4**	**90.6**	**81.6**
Throughput, kbit/s [Note 2]	**181**	**170**	**174**	**157**
No. of complex multiplies/data block(N_m)	67194	204653	40258	115291
No. of complex multiplies / symbol	146	471	144	456
No. of complex multiplies / second	30224920	91600080	28702080	81861120
Approx. MFLOPS needed for DFE implementation	**156**	**458**	**155**	**442**

Note 1: Calculated as D/(N_t + D), the percentage of symbols used for transmitting data vs the total number of symbols transmitted.

Note 2: Assumes an overall code rate of 0.4375, as in the VOA/JPL system with concatenated rate-0.5 convolutional code plus (160,140) Reed-Solomon block code.

Table 6.2: Single carrier system parameters (QPSK, symbol rate fixed at 220 ksymbol/s)

For calculation of the Doppler shift, a maximum vehicle speed of 100 km/h was assumed for both frequency bands. The impact of higher speeds is easily seen by comparing the L-band and S-band cases. The figures in the table for S-band would correspond to an increase of maximum vehicle speed to 159 km/h at L-band. Again, the impact would be to lower the efficiency and throughput. For example, in the 128 μsec maximum delay spread case, the throughput at L-Band would drop from 170 kbit/s to 157 kbit/s. It is interesting to note the similarity in efficiency to the multi-carrier system (i.e., about 80% due to the presence of the guard interval) in this case.

In terms of practical implementation, the computational requirements for the smaller maximum delay spread are within the range of modern high-end DSP chip capabilities. The larger delay spread range requires about three times the computing power, which is somewhat beyond the current state of the art for single-chip floating point DSP's, but DSP technology is continuing to advance at a rapid pace (also, the equalizer could be implemented with fixed-point DSP, albeit with considerably more effort, and fixed-point devices offering up to 1600 MIPS have recently become available).

Implementation of a high-performance equalizer-based receiver seems feasible for the narrowband case with practical delay spread scenarios. The biggest obstacle for such a system will be dealing with flat fading situations, which can be expected to occur fairly frequently (see Section 6.3.1) when the signal from a single transmitter predominates, or in locations where signals from multiple transmitters arrive with nearly identical delays. To ensure adequate fade margins, relatively high gap-filler transmitter powers may be needed, but this will tend to increase the maximum delay spreads outside of their intended coverage areas. The same rules as determined in the case study for multi-carrier modulation to avoid uncovering part of the satellite coverage area around a terrestrial repeater will apply in this case also, therefore reducing the potential reach of the repeater. The use of a diversity antenna system at the receiver is an effective method for combating flat fading, but it may be impractical for portable receivers and tends to be unpopular with car manufacturers.

6.3.4 Case study: wideband single carrier system

For this case, we use the basic characteristics of the WorldSpace system (see Table 6.1). The modulation and coding are similar to that of the narrowband system of the previous section, but the channel symbol rate is greater, by a factor of 7.85. The data rate in this case would be sufficient to carry a flexible multiplex of different audio and data services. The bandwidth is similar to that of the Eureka system, and would hence carry the same benefit of reduced likelihood of flat fading.

	L-Band		S-Band	
Max delay spread, μs	64	128	64	128
No. of equalizer taps (N_{ct})	114	227	114	227
Symbols/channel probe block (N_t)	227	453	227	453
Max. Doppler shift, Hz (@ 100 km/h)	134		213	
Correlation time, ms (T_c)	7.45		4.54	
T_c / T_s	13163		8021	
Channel sampling interval, symbols (N_t + D)	3949		2406	
Data block size, symbols (D)	3722	3496	2179	1953
Efficiency, % [Note 1]	**94.2**	**88.5**	**90.5**	**81.2**
Throughput, kbit/s [Note 2]	**1457**	**1368**	**1400**	**1255**
No. of complex multiplies / data block (N_m)	24732190	88099426	14269107	47472236
No. of complex multiplies / symbol	6645	25201	6549	24308
No. of complex multiplies / second	11060695530	39409197800	10472735120	34877215630
Approx. GFLOPS needed for DFE implementation	**66**	**236**	**63**	**209**

Note 1: Calculated as D/(N_t + D), the percentage of symbols used for transmitting data vs the total number of symbols transmitted.
Note 2: Assumes an overall code rate of 0.437, as in the WorldSpace system with concatenated rate-0.5 convolutional code plus (255,223) Reed-Solomon block code.

Table 6.3: Single carrier system parameters (QPSK, symbol rate fixed at 1.767 Msymbol/s)

However, the complexity calculations for the BDFE, as shown in Table 6.3, reveal a major problem - even for the least complex case, we need computing power of the order of 63 *Giga*FLOPS! This is well beyond the state of the art for DSP chips for the foreseeable future. The major problem is the huge number of taps required in the DFE for the wideband signal.

6.3.5 Discussions

There is a dramatic difference between the feasibility of equalizer-based receivers for the narrowband and wideband implementations of single carrier systems which we have considered. It is to be noted that all the principles and limits described in Section 5 in the case of multi-carrier modulation regarding the number of repeaters required still apply here for the case where the extent of the equalization window ('max.delay spread' indicated in Table 6.3) is equivalent to the size of the guard interval considered in section 5. In the narrowband case, the current (or near future) DSP state of the art appears to be adequate for implementation of a satellite broadcasting system with on-channel terrestrial repeaters, for the maximum delay spreads which we have specified. However, performance of the narrowband system may be unsatisfactory in some locations due to flat fading unless diversity reception techniques are applied, and this presents implementation problems for portable and vehicular receivers. For the same level of receiver complexity, the S-band implementation would have lower throughput than for the L-band case, but the differences are relatively small.

In contrast to the narrowband system, a wideband single carrier system carrying multiple high data rate audio and data services does not appear to be feasible at either 1.5 GHz or 2.3 GHz, unless the delay spreads can be controlled to very small values which is very difficult in the case of on-channel repeaters augmenting a satellite coverage. A practical high-performance equalizer implementation could eliminate ISI for delay spreads up to only a few microseconds. It is difficult therefore to see how a wideband single carrier system could ever be deployed in a practical system in conjunction with terrestrial on-channel repeaters.

7. Impact of carrier frequency

The impact of the carrier frequency on these various system parameters in the case of a hybrid satellite/terrestrial DARS operation has been studied for a number of years in the ITU-R. Table 5.1 of the Special Publication on DSB [ITU-95b] gives a very good summary of the situation as it was understood in 1994. This table has been reproduced here as Figure 7.1 as a reference from which our discussion can be based.

Frequency (GHz)		1.5	2.0	2.5
BSS on-channel gap-filler coverage radius for *C/I= 15.5* dB [a) b) c)]	(km)	3.3	2.5	2.0
BSS fade allowance relative to fade at 1.5 GHz (= 5 dB)	(dB)	0	1	1.8
Effective receiving antenna aperture relative to that at 1.5 GHz (antenna gain = 5 dBi)	(dB)	0	-2.5	-4.5
Receiving system figure of merit	($dB(K^{-1})$)	-22.2	-24.7	-26.7
Beamwidth = 1° Satellite power [d)]	(W)	56	123	233
Antenna diameter	(m)	14	11	9
Beamwidth = 1.6° Satellite power [d)]	(W)	148	315	594
Antenna diameter	(m)	9	7	5.4
Beamwidth = 3.5° Satellite power [d)]	(W)	695	1516	2820
Antenna diameter	(m)	4.1	3.1	2.5
Distance between omnidirectional BS on channel coverage extenders [a) b) c)]	(km)	10.0	7.5	6.0
BS fade allowance relative to fade at 1.5 GHz (= 12 dB)	(dB)	0	2	3.8
Effective receiving antenna aperture relative to that at 1.5 GHz (antenna gain = 0 dBi towards horizon)	(dB)	0	-2.5	-4.5
Receiving system figure of merit	($dB(K^{-1})$)	-27.2	-29.7	-31.7
ERP[e] of main transmitter				
Coverage radius = 33 km; E=100m [f)]	(kW)	21	56	136
Coverage radius = 50 km; E = 150 m [f)]	(kW)	150	402	916
Coverage radius = 64 km; E = 150 m [f)]	(kW)	1354	3666	8319

Notes to Table 5.1:-

a) The transmission mode assumed is Mode II with 62 µs guard interval.

b) For system parameters resulting in equivalent loss of 1 dB caused by Doppler shift in a vehicle moving at 100 km/h.

c) The coverage radius can be considerably higher in the case of repeaters using different frequencies but more spectrum will be required.

d) Powers are for a useful multiplex bit rate of 1,150 kbit/s.

e) Terrestrial station ERP's are for useful multiplex bit rate of 1,150 kbit/s. These ERP's correspond to the same receiver system noise temperature as for the satellite case but with 0 dBi antenna gain, 3 dB interference allowance and no allowance for the feeder-link noise contribution are assumed. The ERP's were calculated referenced to the center of the UHF frequency band, using the F(50,50) propagation curves for 10 m above ground level. A correction factor of 11 dB was applied to bring this height to 1.5 m, more typical of vehicular reception. ERP's at higher frequencies were obtained through frequency scaling assuming the square root of the ratio of frequencies based on fade allowance of 12 dB at 1.5 GHz. The applicability of this scaling to terrestrial broadcasting requires further study.

f) E = Effective height above average terrain of the transmitting antenna i.e., EHAAT.

Table 7.1: Variation of system parameters as a function of frequency for Digital System A (EU-147) (similar values apply to Digital System B (VOA/JPL))

As can be seen in the table, the coverage radius of the on-channel terrestrial gap-filler is indicated to be inversely proportional to the frequency, therefore directly related to the extent of the guard interval. As was found in Section 5.2, the limitation in coverage will respond to more complex rules, especially with respect to a limitation in the ERP of the repeater to avoid uncovering an area of the

satellite coverage due to interference from the terrestrial repeater (directional antennas would help in this case within the limit imposed by back scattering from the buildings). The other cause of a reduction of coverage radius as the increased propagation losses with an increase in frequency as described in Section 4.3.3.

The fade allowance is based on the rule of thumb developed by Goldhirsh and Vogel [GOL-92] which related fading beyond the reduction in effective antenna aperture (20 log F) as the square root of frequency. This seems to be a bit conservative compared to our findings in Section 4.3.2 if a fade allowance of 5 dB is assumed at 1.5 GHz.

The reduction of effective antenna aperture is given relative to 1.5 GHz and results in a reduction of the receiver figure of merit as a function of frequency. This, along with the increase in fade allowance, results in the satellite power figures indicated in the table for various beamwidths. The other element of importance for which frequency has a major impact is the size of the satellite antenna which is related linearly with the frequency. In decreasing the frequency, the satellite antenna diameter increases to a point where a solid reflector can no longer be fitted in the shroud of a launcher. Deployable antenna technology therefore needs to be envisaged with the resulting increased complexity.

Values are also given for the terrestrial case which are also indicative of the operation of the terrestrial repeaters, complementing a satellite service. Parameters such as the distance allowed between repeaters and the expected attenuation on the terrestrial path will also be critical in determining the number of repeaters required to cover a given area. The distance between onmidirectional repeaters is strictly related to the linear scaling of the guard interval with respect to frequency to keep a constant robustness of the system against Doppler spread. In the case of the single-carrier modulation with time-domain equalization, this distance is directly related to the correction window implemented in the equalizer and therefore to the increased complexity of this equalizer. The fade allowance indicated in the table seems to be conservative compared to the findings of Section 4.3.3. Again, the receiver figure of merit will be affected by the reduction in the effective antenna aperture.

The current study has resulted in a number of refinements in the understanding of the effect of the carrier frequency on the various parameters involved in the operation of a satellite DARS complemented by terrestrial on-channel repeaters. Because of the somewhat limited extend of this study, these refinements in the understanding of the various factors involved are more qualitative than quantitative at this stage. This is summarized in Figure 7.1. This figure gives the trends as a function of frequency for the key elements of a satellite/terrestrial DARS operation.

First, the satellite power will have to increase with frequency, as depicted by Curve A due to the reduction in antenna aperture and increased absorption by trees and reduced diffraction at the edge of buildings. The factor between 1.5 GHz and 2.3 GHz was found to be 6 dB in Section 4.3.2. This Curve A increases slightly at lower frequencies since the satellite power would have be increased to compensate for the increase in "man-made" noise. The counter part of this first curve will be an increase in complexity and size of the satellite antenna and feed structure with a lowering in frequency. This is depicted by three Curves, B, B' and B": the first one giving the increased complexity for ¼ CONUS coverage based on time zones; the second one for ½ CONUS; and the third one for a full CONUS coverage, being more relaxed in terms of frequency because of the increased size of the beams resulting in a reduced size of the antenna reflector.

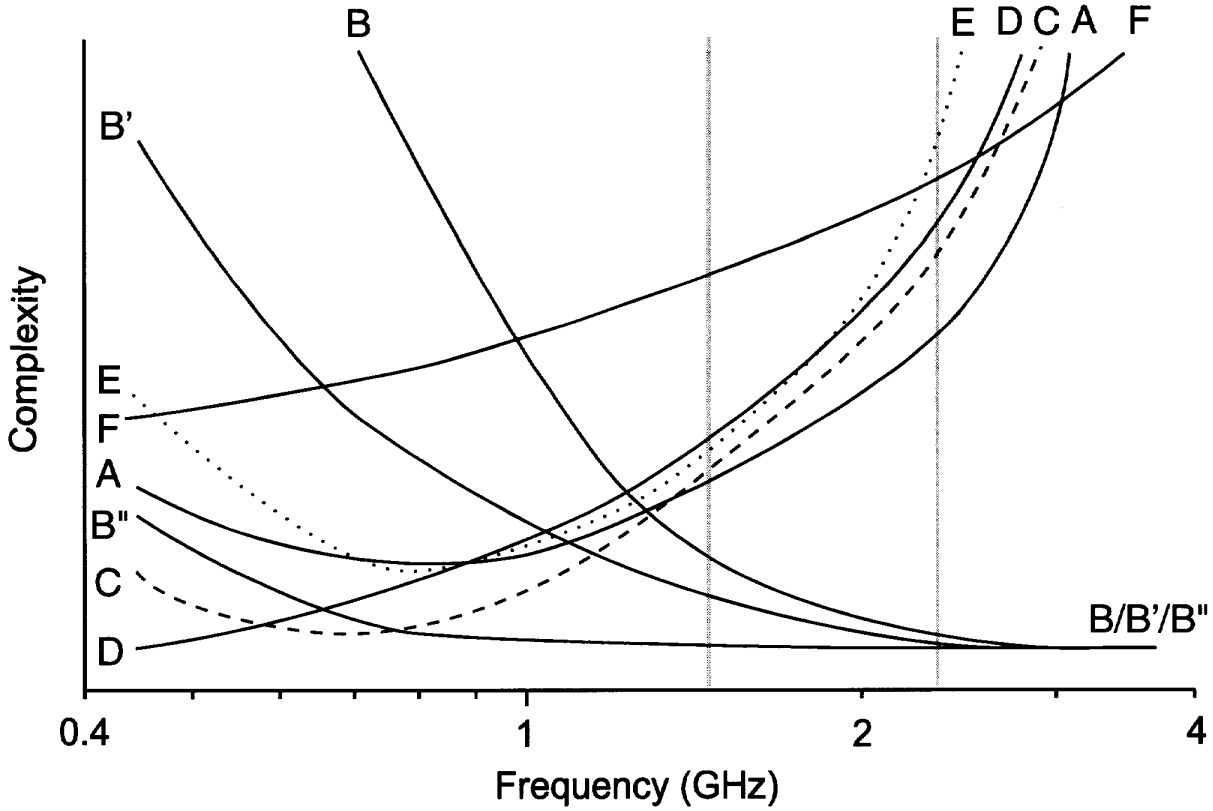

Curve A: Satellite power consideration
Curve B: Satellite antenna size consideration for quarter CONUS (single time zone)
Curve B': Satellite antenna size consideration for half CONUS
Curve B": Satellite antenna size consideration for full CONUS
Curve C: Terrestrial repeater with off-air pick-up consideration
Curve D: Terrestrial repeater with parallel feed structure (SFN) consideration
Curve E: Hybrid satellite/terrestrial repeater with RF pick-up from the satellite
Curve F: Single carrier modulation with channel equalizer

Figure 7.1: Qualitative trade-off summary of system complexity vs carrier frequency

Second, the terrestrial side of the hybrid DAR system is ruled by a number of constraints related to the carrier frequency. The main one is that the system has to work adequately in a Rayleigh channel environment experiencing Doppler spread. Reception has to be protected for vehicular speeds of up to, say, 80 km/h in a city. This calls for a reduction in the extent of the guard interval with an increase in frequency in the case of the multi-carrier modulation. This, in turn, results in an increase in the density of the repeaters as a function of the square of the frequency. Curve C depicts this tendency in increased complexity to cover a given area with terrestrial repeaters picking up signal off-air from each other. Curve D depicts the same aspect with some more complexity added due to the fact that, in this case, a parallel feeder infrastructure to create synchronous Single Frequency Networks (SFN) is assumed.

At lower frequencies, depending whether these repeaters are fed through a parallel infrastructure to create a SFN (for which the complexity decreases constantly with frequency, see curve D), or fed from RF pick-up from the neighboring repeaters, in which case the complexity curve decreases more rapidly but increases again at lower frequencies (Curve C) because of the increased difficulty in securing proper isolation at the on-channel repeater due to limitations at lower frequencies in antenna back-lobe rejection and reflections from the surrounding.

Finally, the coupling of the satellite portion to the terrestrial portion of the system in a hybrid operation has restrictions in terms of the carrier frequency due to the reduction of the guard interval at higher frequency which tends to reduce the power allowed at the terrestrial repeaters to avoid uncovering part of the satellite coverage area. In this case, the restriction is more pronounced as found in Section 5.2.1. This is depicted in Curve E of Figure 7.1. The curve also indicates an increase in complexity at lower frequencies due to the difficulty in securing adequate isolation at the terrestrial repeater since the RF level that will need to be amplified for re-broadcast will be extremely low, as received from the satellite. The repeater RF gain will therefore need to be higher, leading eventually to more likely instability and feedback.

Curve F gives a qualitative assessment of the variation in complexity in the case of the time-domain equalizers needed in the receivers for single carrier modulation systems. As found in Section 6, the increased Doppler spread experienced at higher frequency, which translates for an equalizer into a shorter adaptation time to correct for the channel frequency selective distortion, results in a reduction in throughput of the transmission channel due to the increased need for channel training sequences as well as in an increase in complexity of the equalizer itself expressed in Megaflops. It was found that equalization in this frequency range is only possible with narrowband transmissions (i.e., about 175 kbit/s in L-band and 160 kbit/s in S-band). The ultimate effect of an increase in carrier frequency is therefore a reduction of the feasible channel capacity and bandwidth. Such reduction in bandwidth, unfortunately results in a transmission that is more susceptible to flat fading in a multipath environment than a wideband transmission. Space diversity at the receiver would therefore be required to alleviate this problem. This is why curve F on Figure 7.1 indicates a consistently higher complexity in this case as compared to the multi-carrier modulation case in the range of interest.

In summary, this Figure 7.1 gives a qualitative view of the various factors involved in the operation of a hybrid satellite/terrestrial DAR operation. This figure gives an assessment of the appropriate frequency ranges that can be used for a hybrid satellite/terrestrial DARS system to provide seamless coverage to large service areas such as full CONUS, ½ CONUS and ¼ CONUS. In the case of the full CONUS coverage, the frequency can span a range from 400 MHz to about 2.5 GHz, with the optimum being approximately 600 MHz; as for the ½ CONUS coverage, the frequency can span a range from 600 MHz to about 2.5 GHz with an optimum value of approximately 1 GHz; finally in the case of the ¼ CONUS, the range goes from 800 MHz to about 2.5 GHz with the optimum point being around 1.3 GHz.

Although the system is expected to be feasible over the ranges indicated, the complexity would be minimal around the optimal frequencies. Such complexity would increase towards both extremities of the frequency ranges, especially towards the upper limit due to the large number of factors which, together, will tend to render the feasibility of such a hybrid system excessively difficult.

8. Conclusion

It has been established that, in order to provide a "seamless" coverage in all reception conditions, a satellite DARS system has to be complemented by terrestrial transmitters. In order to make the most efficient use of the RF spectrum and avoid the receiver hunting for the broadcast program on different frequencies, the use of on-channel terrestrial repeaters is preferable. These on-channel repeaters create an especially difficult multipath environment that makes reception of the signal especially challenging, in particular in the case of mobile reception where the time variability of the channel adds to this difficult situation. The carrier frequency used to deliver the DARS signal through satellite as well as terrestrial repeaters has a major impact on the feasibility of such implementation.

A number of elements have been identified throughout this study which are affected by the carrier frequency used. First of all, from the propagation point of view, there is a 4 dB loss due to the reduction of the effective area of the receiving antenna between 1.5 GHz and 2.3 GHz. On top of that, there is another 2 dB loss on the satellite path estimated by the various propagation models investigated in Section 4.3. There is therefore an additional requirement in satellite power at higher frequencies which makes it difficult to include a reasonable fade margin for satellite reception and therefore begs even more for terrestrial gap-fillers to meet the "seamless coverage" requirement.

The other major effect of an increase in carrier frequency is the increase in Doppler spread (linearly related to frequency) which makes the situation more difficult for the digital modulation employed -- either the single carrier modulation with adaptive equalization which has to react more quickly to more rapid channel variations in a multipath context, or the multi-carrier modulation typified by the COFDM. In the case of the channel equalizer, this translates into increased overhead to train the channel equalizer for more rapid changes. It was found that channel equalizers allowing reception of transmission channel wider than about 200 kHz in the context of a hybrid satellite-terrestrial operation in either L-band or S-band are not technically feasible with current technology. In the case of the COFDM, an increase in variability of the channel at higher frequency results in a requirement for a shorter guard interval which limits the free distance between terrestrial repeaters and also limit the maximum power that can be used by these terrestrial repeaters before it starts to affect the satellite coverage in the neighboring areas.

This study looked at typical cases where all these constraints come into play. Depending on the various factors used, the free distance between the terrestrial repeaters can be the limiting factor; in this case, the increase in number of repeaters goes as the square of the ratio in frequency $(2.3/1.5)^2 = 2.35$. This is the most simple case. In fact, the limitation in power for these repeaters to avoid uncovering part of the neighboring satellite coverage proves to be more restrictive. Since the guard interval has to be shorter at higher frequency, the distance at which the signal from the terrestrial repeater becomes destructive for the satellite reception is much shorter and the power allowed at the repeater has to be reduced, resulting in a decrease in the reach of these repeaters. Added to that is the additional propagation effect at higher frequency (some 10 dB additional loss at 2.3 GHz as compared to 1.5 GHz in the terrestrial case). On total, the reach of these terrestrial repeaters is much reduced and therefore results in a higher requirement in density and thus in a larger number of actual repeaters needed for a given service area. The ratios between the number of repeaters required at 2.3 GHz and 1.5 GHz for the cases where omnidirectional terrestrial repeaters and directional repeaters are used are 5.7 and 2.75 respectively.

A figure was developed that summarizes, in a qualitative manner, the various elements that come into play when considering the operating frequency for DARS. In the case of a ¼ CONUS coverage, there seems to be a window between about 800 MHz and 2.5 GHz, with the optimum frequency being around 1.3 GHz, where satellite DARS systems are found to be feasible. This is therefore the best frequency range to accommodate such a hybrid system, with the lowest system complexity expected to be around the optimum frequency. When one gets close to the extremes of this range, the complexity increases rapidly especially toward the upper end of the range, as indicated in Figure 7.1, where many factors seem to converge to render the feasibility of such a hybrid system excessively difficult.

As can be seen, this is a first attempt at rationalizing this complex multi-parameter trade-offs analysis and further work will be needed to refine it further.